Journal of Cluster Science (2022) 33:1387–1397
https://doi.org/10.1007/s10876-021-02063-y

ORIGINAL PAPER

The Application of Encapsulated Trinuclear Cobalt Cluster Complex in Y Zeolite in the One-Pot Multi-Component Synthesis of Spiro Indoline Derivatives

Seyedeh Fatemeh Hojati[1] · Atefeh Sadat Kaheh[1] · Maryam Moosavifar[2] · Fatemeh Daghestani[1]

Received: 7 July 2020 / Accepted: 2 April 2021 / Published online: 16 April 2021

Abstract

A trinuclear cobalt cluster complex was prepared into the nanocages of dealuminated Y zeolite ($[Co_3(O)(CH_3COO)_6(py)_3]$-DAZY) and characterized by XRD, FT-IR, EDS, FE-SEM, AAS and BET-BJH analyses. The elemental content of Cobalt in $[Co_3(O)(CH_3COO)_6(py)_3]$-DAZY was estimated to be about 5.5 mg/g support on the basis of atomic absorption spectroscopy. The catalytic activity of $[Co_3(O)(CH_3COO)_6(py)_3]$-DAZY was evaluated in the synthesis of tri series of spiro indoline derivatives in a library synthesis via the condensation of isatins, malononitrile or ethylcyano acetate, and active methylene compounds (4-hydroxycoumarine, dimedone and pyrazoline-5-one). Corresponding products were obtained in good to excellent yields. Short reaction time, high yield of product, structural diversity of products, absence of organic solvents and the use of water as a green solvent, non-toxicity, stability and reusability of the catalyst are noteworthy advantages of the current work.

Keyword Dealuminated Y zeolite · Encapsulation · Multi-component reaction · Trinuclear metal cluster · Spiro indoline

Introduction

Spiro compounds composed of biologically active heterocycles have been recently gained special attention because they are found in many pharmaceutically active and naturally occurring compounds [1]. Spiro indolines are found in the structure of some known alkaloids and pharmaceuticals such as pteropodine and gelsemine [2–4]. The cytostatic alkaloids such as spirotryprostatins and pteropodines are characteristic examples that are effective inhibitors of microtubule activity and modulators of the function of muscarinic serotonin receptors [5]. It is found that spiro indoline derivatives exhibit extensive biological properties such as antimicrobial [6], antitumor [7], and therapeutic agents [8].

One of the most interesting ring fused to the spiro indoline system is pyran heterocycle because it is an excellent pharmacophore. Spasmolytic, diuretic, anticoagulant, anticancer, and antianaphylactic activities are some biological properties that have been detected for pyran derivatives. [9, 10]. There are several reports for the three-component synthesis of spiro indoline pyranes from the condensation of isatin, active methylene compound and malononitrile. Different reagents and reaction conditions have been used including $InCl_3$ in refluxing acetonitrile or $InCl_3/SiO_2$ under microwave irradiation [11], triethylbenzylammonium chloride (TEBA) [12], boron nitride (BN)@Fe_3O_4 [13], α-Amylase [14], β-cyclodextrin [15], tetra-*n*-butylammonium fluoride (TBAF) [16], Fe_3O_4@L-arginine [17], Cu(II)-β-cyclodextrin [18], KBr [19], borax [20], *N,N*-dimethyl-*n*-octylammonium camphor-10-sulfonate [21], silica propyl imidazolium chloride ([Sipim]Cl) [22], $CuFe_2O_4$ NPs [23] and polystyrene@GO-Fe_3O_4 [24]. Although, some of these methods are valuable, most of them suffer from disadvantages such as long reaction

✉ Seyedeh Fatemeh Hojati
hojatee@yahoo.com; sf.hojati@hsu.ac.ir

[1] Department of Chemistry, Hakim Sabzevari University, Sabzevar 96179-76487, Iran

[2] Department of Chemistry, University of Maragheh, Maragheh 55181-83111, Iran

times, low yields of products, harsh reaction conditions, the use of toxic/non reusable/expensive reagents and toxic solvents. Therefore, the development of new catalytic process for easy access to these pharmacological active compounds is desirable.

There are several methods for the preparation of heterogeneous catalyst. The heterogeneous catalysts satisfactorily use in a various organic transformations and have found some other applications in diverse fields of sciences [25–31]. Encapsulation is one of the best methods for heterogenization of the catalyst. Encapsulation of metal cluster complex in the nanopores of a zeolite makes good catalytic systems that are similar to metalloenzymes and proteins in biochemical transformations [32–34]. In this systems, the metal cluster complex acts as enzyme active sites and the zeolite play the role of protein. Several reports have been found for the catalytic behavior of metal cluster complexes encapsulated in zeolite in various organic reactions such as oxidation, hydrogenation, Friedel–Crafts alkylation and alkylaromatic isomerization or disproportionation [35–43]. Recently, a new trinuclear metal cluster of cobalt complex in the nanocages of dealuminated Y zeolite was prepared and was applied in the epoxidation of cyclohexenes satisfactorily [44]. In the following of our previous work [24, 45–53], herein, we wish to report the multi-component synthesis of spiro indoline derivatives from isatins **1**, malononitrile/ethylcyano acetate **2** and 4-hydroxycoumarin /dimedone/pyrazoline-5-one **3** in the presence of trinuclear cobalt complex $[Co_3(O)(CH_3COO)_6(py)_3]$ encapsulated in dealuminated Y zeolite (Fig. 2) in aqueous medium. Since organic solvents have destructive effect on the environment, many efforts have been made to remove organic solvents from the chemical transformations as an important aspect of green chemistry. It was found that in some reactions, aqueous medium provides greater speed and reactivity due to its strong hydrogen bonding [54, 55].

Experimental Section

Materials and Methods

All materials were commercial reagent grade and obtained from Merck, Sigma-Alderich and Fluka Co. The NaY zeolite was purchased from Sigma–Aldrich chemical company and dealuminated using EDTA treatment [56]. FT-IR spectra were obtained in the range 400–4000 cm^{-1} by Shimadzu 435-U-04 spectrometer in KBr pellets. Field Emission Scanning Electron Micrographs (FE-SEM) of the catalyst and the parent zeolite were recorded on a Philips XL30 microscope. The amount of trinuclear metal cluster cobalt complex was determined by an atomic absorption spectrophotometer (Shimadzu, AA-6200). X-ray powder diffraction (XRD) patterns were recorded on an Advanced Bruker D8 diffractometer using Cu-Kα radiation (40KV, 30 mA). The EDS diagram was obtained by a Philips XL30D6792 spectrometer. The specific surface area of the catalyst was estimated using Brunaer–Emmett–Teller (BET)-BARRET–Joyner–Halenda (BJH) analysis on a Quantachrome NOVA 2200 apparatus at liquid nitrogen temperature (77.3 K). ^1H nuclear magnetic resonance (NMR) spectra were recorded on a Bruker AVANCE 300-MHz spectrometer in DMSO-d6 as the solvent.

Preparation of Encapsulated Cobalt Cluster Complex in the Nanocage of Dealuminated Y Zeolite ($[Co_3(O)(CH_3COO)_6(py)_3]$-DAZY)

The dealumination of Y zeolite was performed by EDTA treatment according to reference [56]. Then cobalt cations were incorporated into the dealuminated Y zeolite via ion exchange process. Next, the cobalt complex was formed in the nanocage of dealuminated Y zeolite using Arunkumar procedure [44]. Briefly, in a tow necked round-bottomed flask, Co-DAZY (0.66 g) was suspended in glacial acetic acid (6.7 ml) and stirred for 30 min at room temperature. Next, pyridine (1.3 ml) was added dropwise during 15 min. Then, NaBr (0.22 g) and distilled water (2.5 ml) were added and stirred for 30 min again. Aqueous H_2O_2 (6 ml) was added and stirred at room temperature for 3 h. The pink solid catalyst was filtered, washed with glacial acid, purified with soxhlet extraction and dried at room temperature. The white obtained catalyst includes 5.5 mg/g Co content which was estimated by atomic absorption spectroscopy. However, based on encapsulation of cluster into nanocage of zeolite, the original white color altered to light pink color and it remained unchanged based on soxhlet extraction which proved entering of metal complexes into zeolite cage (Fig. 1).

General Procedure for the Synthesis of Spiro Indoline-3,4′-Pyran Derivatives

A mixture of isatin **1** (1 mmol), 4-hydroxycoumarin/dimedone/pyrazoline-5-one **3** (1 mmol), malononitrile/ethyl cyanoacetate **2** (1 mmol), and $[Co_3(O)(CH_3COO)_6(py)_3]$-DAZY (15 mg) in water (5 ml) was prepared and stirred at 80 °C until the starting materials disappeared. After completion of the reaction as monitored by TLC (eluent: EtOAc/*n*-hexane, 1:1), hot ethanol (10 ml) was added and the reaction mixture was filtered and the residue was washed with ethanol. The filtrate was poured on crushed ice and allowed to form precipitate. The crude solid product **4** was filtered and recrystallized from EtOH to afford the pure products in high purity and yield (Table 2).

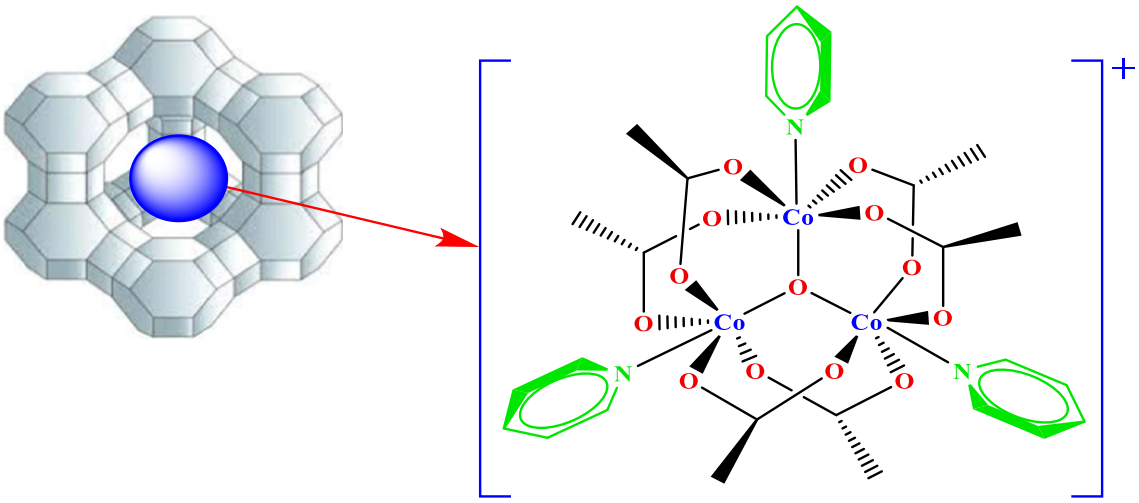

Fig. 1 Trinuclear cobalt cluster complex encapsulated in dealuminated Y zeolite ($[Co_3(O)(CH_3COO)_6\text{-}(py)_3]$-DAZY)

Physical and Spectral Data of Some Products

2′-Amino-5-chloro-2,5′-dioxo-5′*H*-spiro[indoline-3,4′-pyrano[3,2-*c*]chromene]-3′ carbonitrile **4{6,1,1},** mp: > 300 °C. FT-IR (KBr, cm^{-1}): 3319, 3207, 2199, 1741, 1677, 1608, 1475, 1360, 1222, 1090, 972. ^{1}H NMR (300 MHz, DMSO-d_6, ppm): 6.87 (d, *J* = 8.4 Hz, 1H, ArH), 7.25–7.28 (m, 1H, ArH), 7.44 (s, 1H, ArH), 7.50 (d, *J* = 8.4 Hz, 1H, ArH), 7.55 (t, *J* = 7.6 Hz, 1H, ArH), 7.74 (s, 2H, NH_2), 7.78 (d, *J* = 8.4 Hz, 1H, ArH), 7.94 (d, *J* = 7.6 Hz, 1H, ArH), 10.82 (s, 1H, NH).

Ethyl-2′-Amino-2,5′-dioxo-5′H-spiro[indoline-3,4′-pyrano[3,2-*c*]chromene]-3′-carboxylate **4{1,2,1},** mp: 251–254 °C. FT-IR (KBr, cm^{-1}): 3358, 3261, 2981, 1696, 1641, 1514, 1491, 1472, 1396, 1380, 1289, 1135, 1074, 929, 747, 684. ^{1}H NMR (DMSO-d_6, δ, 300 MHz): 0.81 (t, *J* = 7.2 Hz, 3H, CH_3), 3.73–3.77 (m, 2H, CH_2O), 6.71–6.81 (m, 2H, ArH), 7.00 (d, *J* = 6.9 Hz, 1H, ArH), 7.10 (t, *J* = 7.8 Hz, 1H, ArH), 7.42–7.53 (m, 2H, ArH), 7.73 (t, *J* = 8.1 Hz, 1H, ArH), 8.01 (d, *J* = 8.4 Hz, 1H, ArH), 8.13 (br s, 2H, NH_2), 10.42 (s, 1H, NH).

2-Amino-7,7-dimethyl-2′,5-dioxo-5,6,7,8-tetrahydrospiro[chromene-4,3′-indoline]-3-carbonitrile **4{1,1,2},** mp: 290–292 °C. FT-IR (KBr, cm^{-1}): 3377, 3312, 3144, 2192, 1723, 1683, 1656, 1472, 1348, 1223, 1055. ^{1}H NMR (300 MHz, DMSO-d_6, ppm): 1.01 (s, 3H, CH_3), 1.04 (s, 3H, CH_3), 2.10 (d, *J* = 16.0 Hz, 1H, CH_2), 2.18 (d, *J* = 16.0 Hz, 1H, CH_2), 2.54 (d, *J* = 18.0 Hz, 1H, CH_2), 2.59 (d, *J* = 18.0 Hz, 1H, CH_2), 6.79 (d, *J* = 7.6 Hz, 1H, ArH), 6.89 (t, *J* = 7.2 Hz, 1H, ArH), 6.98 (d, *J* = 7.2 Hz, 1H, ArH), 7.14 (t, *J* = 7.6 Hz, 1H, ArH), 7.24 (s, 2H, NH_2), 10.40 (s, 1H, NH).

2-Amino-5′-chloro-7,7-dimethyl-2′,5-dioxo-5,6,7,8-tetrahydrospiro[chromene-4,3′-indoline]-3-carbonitrile **4{6,1,2}**, mp: > 300 °C. FT-IR (KBr, cm^{-1}): 3372, 3290, 3156, 2193, 1726, 1680, 1654, 1602, 1478, 1350, 1225, 1057. ^{1}H NMR (300 MHz, DMSO-d_6, ppm): 1.02 (s, 6H, 2CH3), 2.16 (t, *J* = 16.4 Hz, 2H, CH_2), 2.52 (d, *J* = 18.0 Hz, 1H, CH_2), 2.59 (d, *J* = 18.0 Hz, 1H, CH_2), 6.81 (d, *J* = 8.4 Hz, 1H, ArH), 7.11 (s, 1H, ArH), 7.19 (d, *J* = 8.4 Hz, 1H, ArH), 7.33 (s, 2H, NH_2), 10.55 (s, 1H, NH).

Ethyl-2-Amino-7,7-dimethyl-2′,5-dioxo-5,6,7,8-tetrahydrospiro[chromene-4,3′-indoline]-3-carboxylate **4{1,2,2}**, mp: 256–258 °C. FT-IR (KBr, cm^{-1}): 3372, 3236, 3181, 2956, 1715, 1688, 1670, 1648, 1617, 1526, 1470, 1347, 1316, 1291, 1222, 1166, 1053, 901, 786, 745. ^{1}H NMR (300 MHz, DMSO-d_6, ppm): 0.80 (t, *J* = 7.2 Hz, 3H, CH_3), 0.95 (s, 3H, CH_3), 1.02 (s, 3H, CH_3), 1.96–2.18 (m, 2H, CH_2), 2.46–2.61 (m, 2H, CH_2), 3.63–3.73 (m, 2H, CH_2O), 6.67 (d, *J* = 7.6 Hz, 1H, ArH), 6.76 (t, *J* = 7.2 Hz, 1H, ArH), 6.84 (d, *J* = 7.2 Hz, 1H, ArH), 7.03–7.07 (m, 1H, ArH), 7.87 (br s, 2H, NH_2), 10.15 (s, 1H, NH).

6′-Amino-3′-methyl-2-oxo-1′-phenyl-1′H-spiro[indoline-3,4′-pyrano[2,3-*c*] pyrazole]-5′-carbonitrile **4{1,1,3}**, mp: 239–241 °C. FT-IR (KBr, cm^{-1}): 3412, 3280, 3174, 2200, 1692, 1650, 1526, 1132. ^{1}H NMR (300 MHz, DMSO-d_6, ppm): 1.55 (s, 3H, CH_3), 6.94 (d, *J* = 7.6 Hz, 1H, ArH), 7.03 (t, *J* = 7.6 Hz, 1H, ArH), 7.18 (d, *J* = 7.2 Hz, 1H, ArH), 7.28 (t, *J* = 7.6 Hz, 1H, ArH), 7.37 (t, *J* = 7.6 Hz, 1H, ArH), 7.53 (t, *J* = 8.0 Hz, 2H, ArH), 7.58 (s, 2H, NH_2), 7.81 (d, *J* = 7.6 Hz, 2H, ArH), 10.76 (s, 1H, NH).

6′-Amino-5-chloro-3′-methyl-2-oxo-1′-phenyl-1′H-spiro[indoline-3,4′-pyrano[2,3-*c*] pyrazole]-5′-carbonitrile **4{6,1,3}**, mp: 226–228 °C. FT-IR (KBr, cm^{-1}): 3467, 3305, 3138, 2191, 1736, 1645, 1526, 1476, 1384, 1211, 1072. ^{1}H NMR (300 MHz, DMSO-d_6, ppm): 1.60 (s, 3H, CH_3), 6.96 (d, *J* = 8.4 Hz, 1H, ArH), 7.33–7.36 (m, 3H,

ArH), 7.52 (t, J = 8.0 Hz, 2H, ArH), 7.64 (s, 2H, NH_2), 7.79 (d, J = 8.0 Hz, 2H, ArH), 10.89 (s, 1H, NH).

Ethyl-6′-Amino-3′-methyl-2-oxo-1′-phenyl-1′H-spiro[indoline-3,4′-pyrano[2,3-*c*] pyrazole]-5′-carboxylate **4{1,2,3}**, mp: 235–237 °C. FT-IR (KBr, cm^{-1}): 3381, 3233, 3174, 1718, 1692, 1663, 1612, 1534, 1470, 1353, 1283, 1116, 1030, 966, 762, 678. ^{1}H NMR (300 MHz, DMSO-d_6, ppm): 0.72 (t, J = 7.2 Hz, 3H, CH_3), 1.56 (s, 3H, CH_3), 3.70–3.74 (m, 2H, CH_2O), 6.82–6.96 (m, 3H, ArH), 7.13–7.18 (m, 1H, ArH), 7.32 (t, J = 7.2 Hz, 1H, ArH), 7.49 (t, J = 7.8 Hz, 2H, ArH), 7.78 (d, J = 7.8 Hz, 2H, ArH), 8.20 (br s, 2H, NH_2), 10.50 (s, 1H, NH).

Results and Discussion

After preparation of $Co_3(O)(CH_3COO)_6$ $(py)_3$]-DAZY (Fig. 2) as described in experimental section, the characterization of the catalyst was performed by XRD, FT-IR, EDS, FE-SEM and BET-BJH techniques.

The XRD pattern of dealuminated Y zeolite and $[Co_3(O)(CH_3COO)_6$-$(py)_3]$-DAZY are shown in Fig. 2a, b. These patterns exhibit similar crystallinity for the catalyst and its parent zeolite that proves the framework and crystallinity of the zeolite structure did not change during the cobalt complex formation. Peak in the (220), (311) and (331) is sensitive to replacement of metal. Based on encapsulation, the relative peak intensity changed from (331)> (220)> (311) to (331)> (311)> (220) which prove the encaging of cluster into zeolite cage [57]. However, the appearance of new peak in the region of $2\theta \cong 7.5$ can be related to the presence of complex in zeolite cage.

In the FT-IR spectra of DAZY zeolite (Fig. 2c) and $[Co_3(O)(CH_3COO)_6$-$(py)_3]$-DAZY (Fig. 2d), the peaks at 557, 1022 cm^{-1}, 1637 cm^{-1} and 3444 cm^{-1} belong to the vibration of the internal and external lattice linkages and lattice water molecules respectively [58]. The comparison of FT-IR spectrum of cobalt complex (Fig. 2e) and $[Co_3(O)(CH_3COO)_6$-$(py)_3]$-DAZY (Fig. 2d) exhibits that the bands of cobalt complex in the catalyst spectrum are weak due to its low concentration and were overlapped by the framework vibrations of the zeolite matrix [59]. The absorption bands at 696, 1640, 1550 and 2910 cm^{-1} are related to Co–O–Co, carboxylate anion, C=N and C–H stretching vibrations.

The presence of Co, C and N elements in the $[Co_3(O)(CH_3COO)_6$-$(py)_3]$-DAZY structure were confirmed by EDS analysis. In Table 1, the elemental content of DAZY and the catalyst was compared together on the basis of obtained EDS data.

The FE-SEM micrographs of DAZY and $[Co_3(O)(CH_3COO)_6$-$(py)_3]$-DAZY showed the similar crystalline appearance for both particles. It proves that the cobalt complex formed into nanocages of Y zeolite (Fig. 3).

The BET-BJH analysis was performed using nitrogen adsorption–desorption measurements at 77.3 K to determine the specific surface area, mesopore specific surface area, micropore specific surface area and the size and volume of the pores of $[Co_3(O)(CH_3COO)_6$-$(py)_3]$-DAZY. The results are summarized in Table 2.

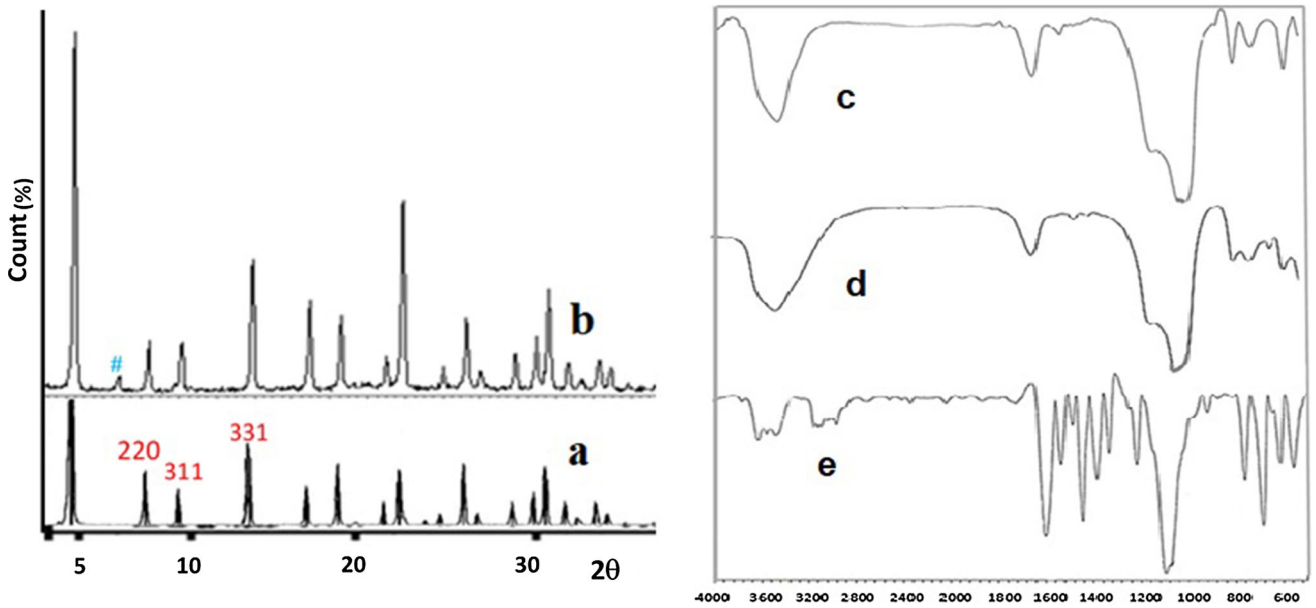

Fig. 2 (a) The XRD patterns of dealuminated Y zeolite and (b) $[Co_3(O)(CH_3COO)_6$-$(py)_3]$-DAZY, (c) The FT-IR spectra of DAZY, (d) $[Co_3(O)(CH_3COO)_6$-$(py)_3]$-DAZY and (e) $Co_3(O)(CH_3COO)_6$-$(py)_3$

Table 1 The EDS analyses of DAZY and $[Co_3(O)(CH_3COO)_6\text{-}(py)_3]$-DAZY

Element	Al (%)	Si (%)	Co (%)	C (%)	N (%)
DAZY	(11.56)	(32.36)	–	–	–
$[Co_3(O)(CH_3COO)_6\text{-}(py)_3]$-DAZY	11.19	31.22	0.53	0.96	0.13

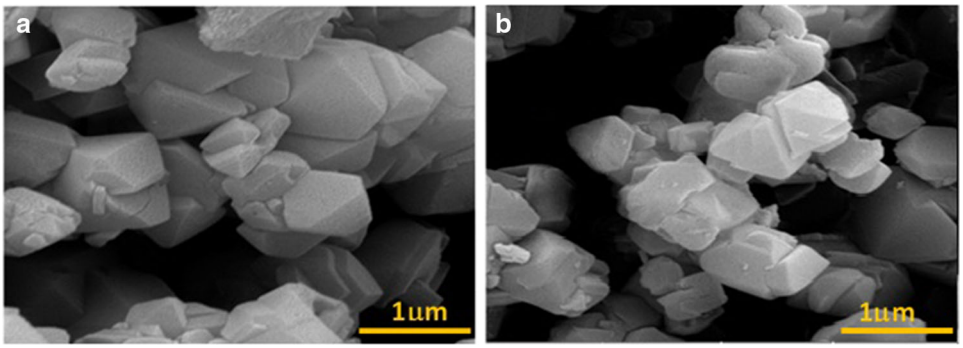

Fig. 3 FESEM image of **a** DAZY and **b** $[Co_3(O)(CH_3COO)_6\text{-}(py)_3]$-DAZY

Table 2 The BET-BJH analyses of $[Co_3(O)(CH_3COO)_6\text{-}(py)_3]$-DAZY

Total specific surface area (m^2/g)	Mesopore specific surface area (m^2/g)	Micropore specific surface area (m^2/g)	Total pore volume (cm^3/g)	Micropore volume (cm^3/g)	Average pore diameter (nm)
504	376.45	127.55	0.34	0.031	0.51

After preparation and characterization of trinuclear cobalt complex encapsulated in the nanocages of dealuminated Y zeolite ($[Co_3(O)(CH_3COO)_6\text{-}(py)_3]$-DAZY), Its catalytic activity was investigated in the three-component synthesis of spiro indoline-3,4′-pyran derivatives. Initially, the reaction of isatin **1{1}**, malononitrile **2{1}**, and 4-hydroxycoumarin **3{1}** was selected as model reaction (Scheme 1).

To optimize the reaction condition, the model reaction was performed in different temperatures and solvents. Water, ethanol, methanol and dimethylformamide at room temperature and also at 50, 80, and 100 °C were examined in the model reaction (Table 3, entries 1–7). It was found that the yield of product **4{1,1,1}** was increased and the reaction time was shortened at 80 °C in water (Table 3, entry 3). The model reaction was also performed in the absence of solvent, that a poor yield was obtained in solvent-free condition (Table 3, entry 8). Furthermore, the amount of required catalyst was optimized in the model reaction that the best result was obtained using 15 mg $[Co_3(O)(CH_3COO)_6(py)_3]$-DAZY and more amount of the catalyst did not improve the product yield (Table 1, entries 8–10). The catalytic activity of DAZY was also considered in the model reaction at 80 °C in water and 53% products was obtained after 30 min (Table 3, entry 11). When the model reaction was carried out without any catalyst under optimized condition, only trace product was detected in the reaction mixture (Table 3, entry 12).

After optimization of the conditions, the generality and the library construction of the optimized method was investigated in the reaction of nine substituted isatins **1{1–9}**, malononitrile, or ethyl cyano acetate **2**{1–2}, and three active methylene compounds **3{1–3}** (Scheme 2). Corresponding spiro indoline-3,4′-pyran derivatives **4** were

Scheme 1 The model reaction catalyzed by $[Co_3(O)(CH_3COO)_6\text{-}(py)_3]$-DAZY

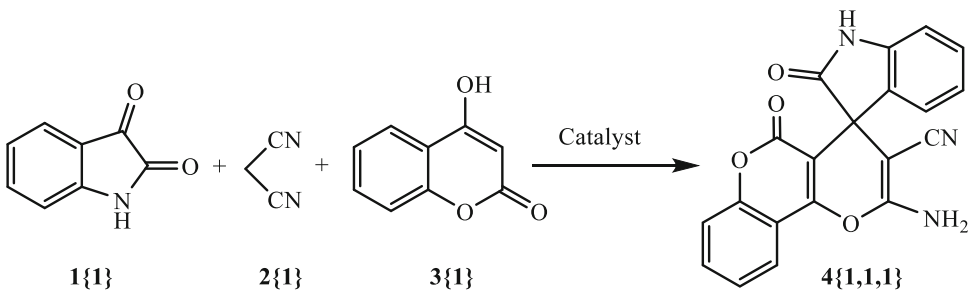

1{1} 2{1} 3{1} 4{1,1,1}

Table 3 Optimization of the reaction condition for the synthesis of product **4{1,1,1}** in the presence of $[Co_3(O)(CH_3COO)_6\text{-}(py)_3]$-DAZY

Entry	Catalyst	Solvent	T (°C)	Time (min)	Yield (%)[b]
1	$[Co_3(O)(CH_3COO)_6\text{-}(py)_3]$-DAZY (15 mg)	H_2O	rt	120	30
2	$[Co_3(O)(CH_3COO)_6\text{-}(py)_3]$-DAZY (15 mg)	H_2O	50	240	60
3	$[Co_3(O)(CH_3COO)_6\text{-}(py)_3]$-DAZY (15 mg)	H_2O	80	30	95
4	$[Co_3(O)(CH_3COO)_6\text{-}(py)_3]$-DAZY (15 mg)	H_2O	100	120	83
5	$[Co_3(O)(CH_3COO)_6\text{-}(py)_3]$-DAZY (15 mg)	EtOH	80	30	20
6	$[Co_3(O)(CH_3COO)_6\text{-}(py)_3]$-DAZY (15 mg)	MeOH	80	30	10
7	$[Co_3(O)(CH_3COO)_6\text{-}(py)_3]$-DAZY (15 mg)	DMF	80	30	–
8	$[Co_3(O)(CH_3COO)_6\text{-}(py)_3]$-DAZY (15 mg)	–	80	30	25
9	$[Co_3(O)(CH_3COO)_6\text{-}(py)_3]$-DAZY (5 mg)	H_2O	80	30	85
10	$[Co_3(O)(CH_3COO)_6\text{-}(py)_3]$-DAZY (10 mg)	H_2O	80	30	90
11	$[Co_3(O)(CH_3COO)_6\text{-}(py)_3]$-DAZY (20 mg)	H_2O	80	30	93
12	DAZY (15 mg)	H_2O	80	30	53
13	–	H_2O	80	30	Trace

[a]The reaction was carried out with 1 mmol of starting materials

[b]Isolated yields

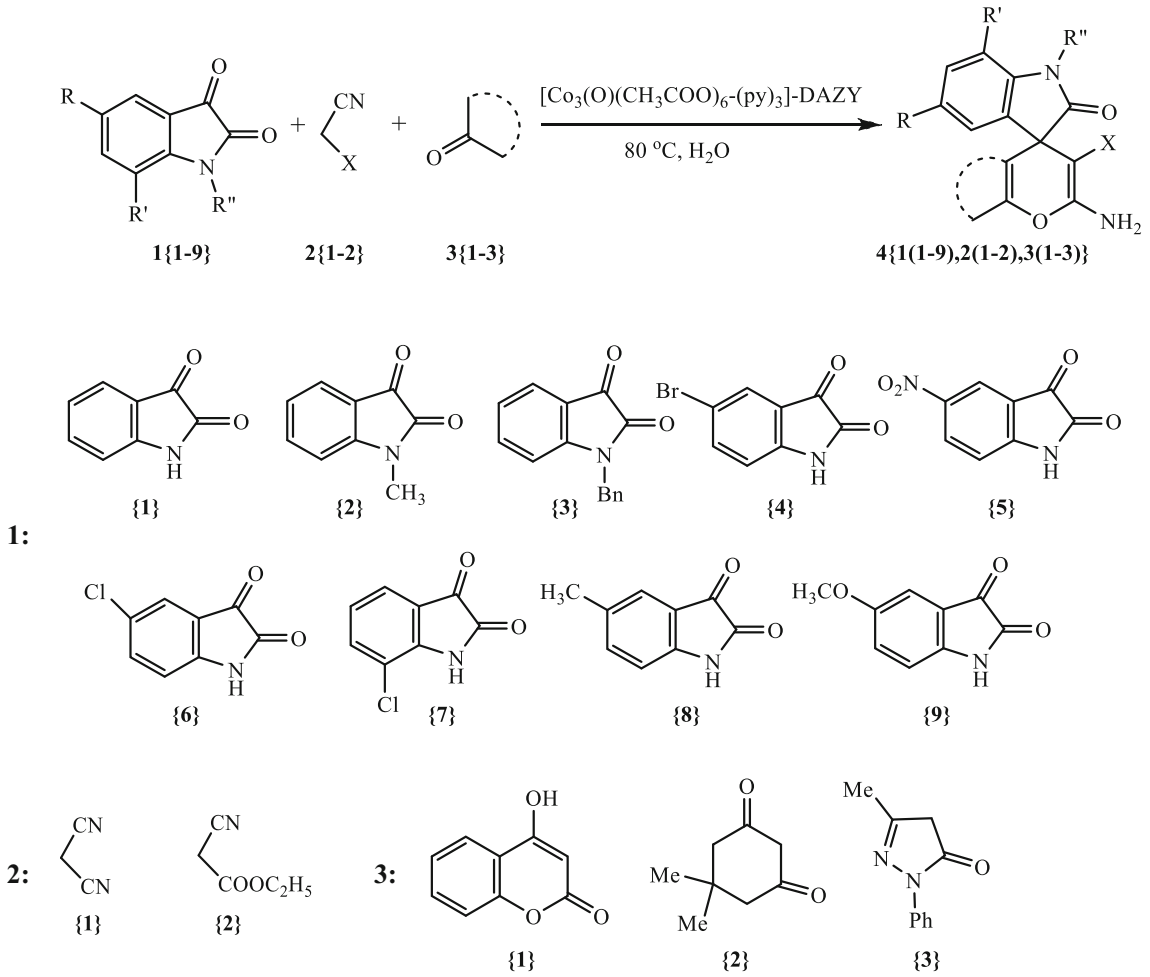

Scheme 2 Synthesis of spiro indoline-3,4′-pyran derivatives using $[Co_3(O)(CH_3COO)_6\text{-}(py)_3]$-DAZY

Table 4 Synthesis of spiro indoline-3,4′-pyran derivatives **4** catalyzed by $[Co_3(O)(CH_3COO)_6(py)_3]$-DAZY

Entry	Products **4**	Time (min)	Yield (%)[a]	Mp (°C)	Lit. Mp (°C) [ref.]
1	**4{1,1,1}**	30	95	> 300	> 300 [22]
2	**4{2,1,1}**	40	94	286–288	286–288 [22]
3	**4{3,1,1}**	35	93	280–282	277–279 [60]
4	**4{4,1,1}**	45	93	> 300	> 300 [61]
5	**4{5,1,1}**	20	96	295–298	> 300 [22]
6	**4{6,1,1}**	25	95	> 300	> 300 [22]
7	**4{7,1,1}**	20	95	> 300	> 300 [60]
8	**4{8,1,1}**	55	88	> 300	> 300 [60]
9	**4{9,1,1}**	20	86	270–272	272–274 [61]
10	**4{1,2,1}**	37	95	251–254	253–255 [22]
11	**4{4,2,1}**	25	88	278–280	280–282 [22]
12	**4{5,2,1}**	25	90	272–274	267–268 [22]
13	**4{6,2,1}**	22	96	280–282	275–278 [22]
14	**4{1,1,2}**	10	95	290–292	289–290 [12]
15	**4{2,1,2}**	20	87	250–252	254–256 [12]
16	**4{3,1,2}**	25	83	267–269	269–271 [12]
17	**4{4,1,2}**	15	80	298–299	> 300 [13]
18	**4{5,1,2}**	17	92	> 300	> 300 [62]
19	**4{6,1,2}**	15	97	295–297	293–295 [63]
20	**4{7,1,2}**	20	97	> 300	> 300 [12]
21	**4{8,1,2}**	15	70	279–281	279–281 [63]
22	**4{1,2,2}**	22	85	280–282	279–281 [63]
23	**4{4,2,2}**	15	70	295–298	296–298 [62]
24	**4{5,2,2}**	20	81	276–279	276–278 [62]
25	**4{6,2,2}**	20	87	292–294	292–293 [63]
26	**4{7,2,2}**	25	87	280–283	278–280 [63]
27	**4{8,2,2}**	20	83	286–289	284–285 [63]
28	**4{1,1,3}**	30	85	239–241	235–237 [22]
29	**4{2,1,3}**	20	70	198–199	200 [11]
30	**4{3,1,3}**	40	40	210–213	214–215 [64]
31	**4{4,1,3}**	25	78	244–246	242–244 [62]
32	**4{5,1,3}**	30	97	226–228	227–229 [22]
33	**4{6,1,3}**	25	70	228–230	232–233 [22]
34	**4{8,1,3}**	30	86	284–286	288–290 [62]
35	**4{1,2,3}**	35	86	236–238	239–241 [22]
36	**4{2,2,3}**	50	75	232–234	224–226 [22]
37	**4{4,2,3}**	40	73	254–256	252–254 [62]
38	**4{5,2,3}**	35	85	269–271	267–269 [22]
39	**4{6,2,3}**	30	88	246–248	246–247 [22]
40	**4{8,2,3}**	35	97	233–236	230–232 [62]

[a]Isolated yield

synthesized in good yields at 80 °C in water in the presences of $[Co_3(O)(CH_3COO)_6$-$(py)_3]$-DAZY. The results are shown in Table 4.

As shown in Table 4, it was found that this procedure is operational for a wide variety of reactants. A series of substituted isatins **1** and different 1,3-dicarbonyl compounds **3** were used in this reaction successfully. Although, the reaction of malononitrile and ethylcyano acetate **2** with other substrates were performed satisfactorily, the reaction time of ethylcyano acetate with isatins **1** and 1,3-dicarbonyl compounds **3** was longer than those of malononitrile **2{1}**, which is probably due to the lower reactivity of the cyanoacetic ester **2{2}**. The results obviously show that the current method is applicable to the synthesis of libraries

with high diversity. We expect this procedure find extensive application in the field of combinatorial chemistry and drug discovery.

The reusability of the catalyst was also studied in the model reaction in the presence of $[Co_3(O)(CH_3COO)_6$-$(py)_3]$-DAZY under optimized condition. After completion of the reaction, hot ethanol was added to the mixture and filtered, washed with ethanol and the separated catalyst dried at 100 °C for 1 h. The recovered catalyst was used in the model reaction again. The FT-IR, XRD and SEM analyses of recovered catalyst has been shown in Fig. 4. The recovery and reuse of the catalyst was successively performed 9 times for the synthesis of **4{1,1,1}** as described in experimental section and the product yields were 95, 95, 94, 93, 93, 92, 92, 92 and 90 after 30 min respectively that show no significant loss of the catalytic activity of $[Co_3(O)(CH_3COO)_6$-$(py)_3]$-DAZY.

A possible mechanism for this synthesis of product **4{1,1,1}** catalyzed by $[Co_3(O)(CH_3COO)_6$-$(py)_3]$-DAZY is proposed in Scheme 3. The catalyst plays an important role in accelerating the reaction due to its Lewis acidity character. It seems that Co ions have the main catalytic role in the reaction mechanism. Co_3O-DAZY including Co^{2+}, Co^{3+} ions and therefore Co^{3+} act as Lewis acid and can provide a nucleophilic attack by activating the electrophilic sites of the reaction. However, DAZY has been used as

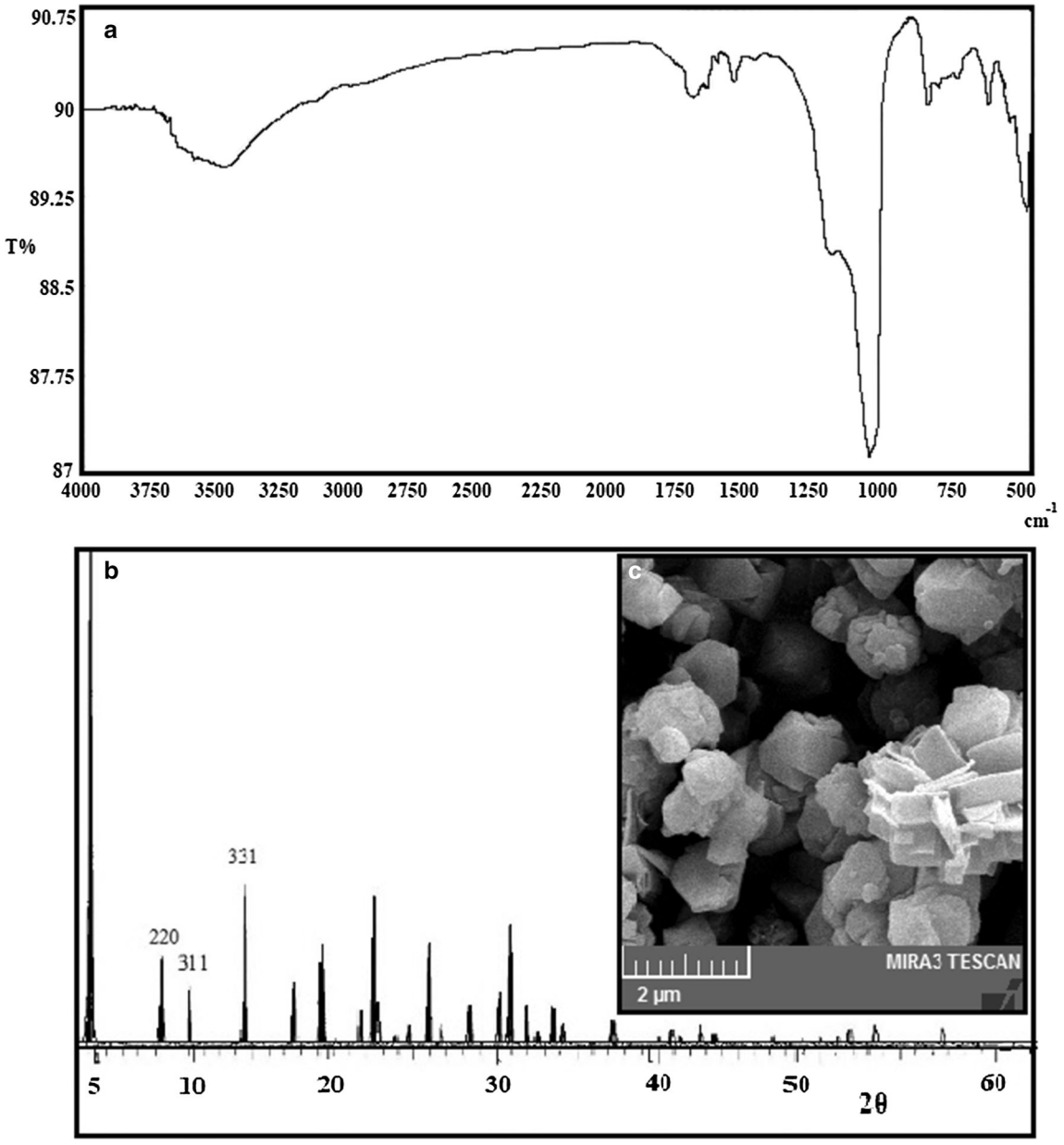

Fig. 4 The FT-IR spectrum (**a**), XRD pattern (**b**) and SEM image (**c**) of recovered catalyst

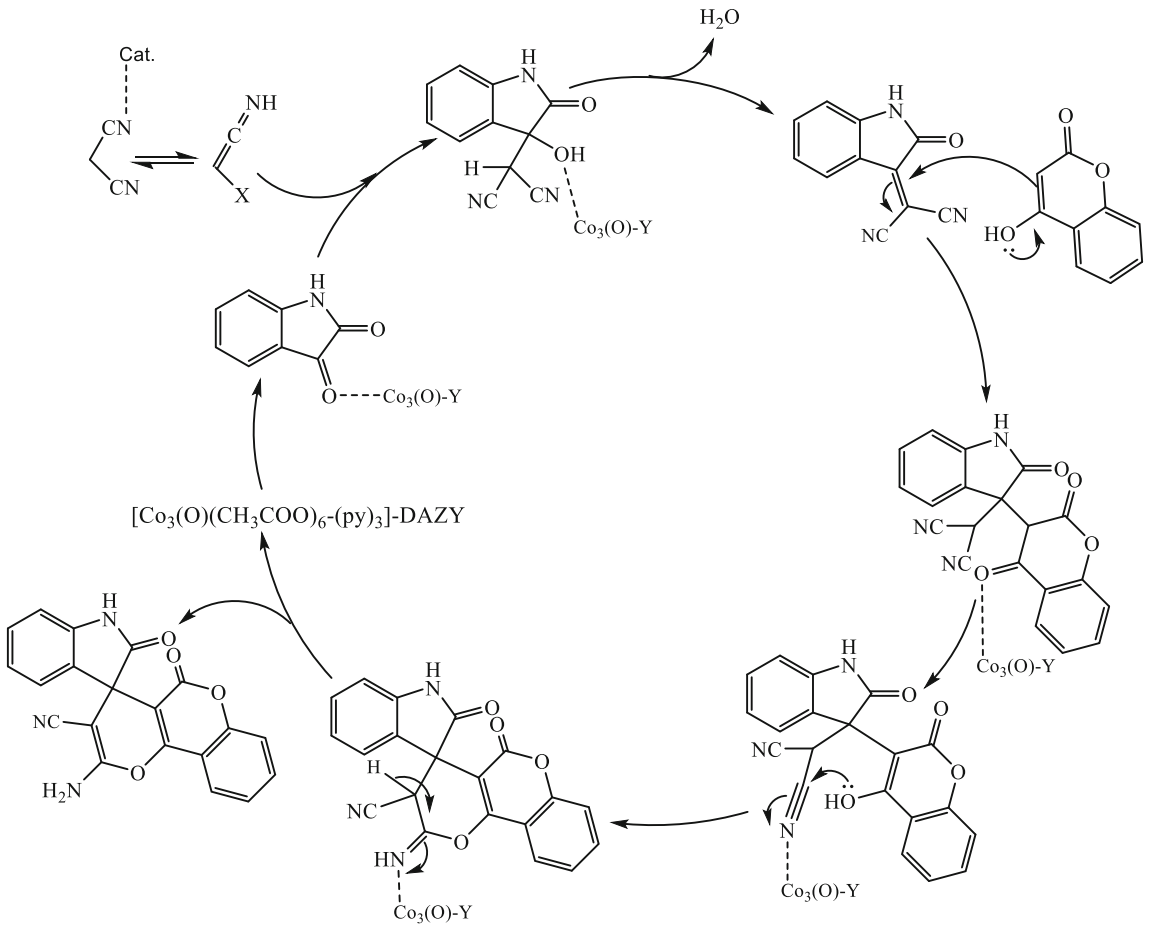

Scheme 3 Proposed mechanism for the synthesis of product **4{1,1,1}** using $[Co_3(O)(CH_3COO)_6\text{-}(py)_3]$-DAZY

support to prevent of deactivation of catalyst (Co cluster). In addition, the Lewis acidity of Y zeolite is less than the catalyst and therefore, it expected that Co_3O-DAZY catalyze the reaction. Furthermore, As described in the results and discussion section, (Table 3, entry 12), the catalytic activity of DAZY was increased by encapsulation of Co cluster complex in zeolite nano cage.

Finally, the present work was compared with some other reported procedure for the synthesis of **4{1,1,1}** in Table 5.

Table 5 Comparison of the previous reported procedure with the current work for the synthesis of spiro indoline-3,4′-pyran

Compound	Condition	Time	Yield (%)
4{1,1,1}	$InCl_3$ (20 mol%), CH_3CN, reflux [11]	1.5 h	74
	TEBA[a] (20 mol%), H_2O, 60 °C [12]	3 h	88
	BN[b]@Fe_3O_4, H_2O, reflux [13]	45 min	88
	α-Amylase (246 U) EtOH:H_2O (9:1), rt [14]	2 days	55
	β-cyclodexterine (100 mol%), H_2O, 60 °C [15]	8 h	88
	Cu(II)-β-Cyclodextrin, EtOH, rt [18]	8 h	80
	Borax, EtOH/Reflux [20]	2 h	91
	$CuFe_2O_4$ NPs, EtOH:H_2O (1:1), reflux [23]	80 min	85
	PS@GO-Fe_3O_4, H_2O, 80 °C [24]	50 min	95
	Sodium stearate (10 mol%), H_2O, 60 °C [60]	3 h	92
	$[Co_3(O)(CH_3COO)_6\text{-}(py)_3]$-DAZY, H_2O, 80 °C [This work]	30 min	95

[a]Triethylbutylammonium chloride

[b]Boron nitride

Conclusions

Encapsulated trinuclear cobalt cluster complex in dealuminated Y zeolite was prepared and characterized by XRD, FT-IR and FE-SEM analyses. This catalyst was evaluated in the synthesis of tri series of spiro indoline derivatives in a library synthesis and corresponding products were obtained in good to excellent yields. Short reaction time, high yield of product, structural diversity of products, absence of organic solvents and the use of water as a green solvent, non-toxicity, stability and reusability of the catalyst are noteworthy advantages of the current work.

Acknowledgements The authors thank Hakim Sabzevari University for the financial support of this work.

References

1. A. Longeon, M. Guyot, and J. Vacelet (1990). *Experientia* **46**, 548–550.
2. F. Zhou, Y. L. Liu, and J. Zhou (2010). *Adv. Synth. Catal.* **352**, 1381–1407.
3. R. M. Williams and R. J. Cox (2003). *Acc. Chem. Res.* **36**, 127–139.
4. Y. M. Litvinov, V. Y. Mortikov, and A. M. Shestopalov (2008). *J. Comb. Chem.* **10**, 741–745.
5. T. H. Kang, K. Matsumoto, Y. Murakami, H. Takayama, M. Kitajima, N. Aimi, et al. (2002). *Eur. J. Pharmacol.* **444**, 39–45.
6. G. Bhaskar, Y. Arun, C. Balachandran, C. Saikumar, and P. T. Perumal (2012). *Eur. J. Med. Chem.* **51**, 79–91.
7. X. Jiang, Y. Sun, J. Yao, Y. Cao, M. Kai, N. He, X. Zhang, Y. Wang, and R. Wang (2012). *Adv. Synth. Catal.* **354**, 917–925.
8. C. V. Galliford and K. A. Scheidt (2007). *Angew. Chem. Int. Ed.* **46**, 8748–8758.
9. L. L. Andreani and E. Lapi (1960). *Boll. Chim. Farm.* **99**, 583–586.
10. L. Bonsignore, G. Loy, and D. Secci (1993). *Eur. J. Med. Chem.* **28**, 517–520.
11. G. Shanthi, G. Subbulakshmi, and P. T. Perumal (2007). *Tetrahedron* **63**, 2057–2063.
12. S.-L. Zhu, S.-J. Ji, and Y. Zhang (2007). *Tetrahedron* **63**, 9365–9568.
13. A. Molla and S. Hussain (2016). *RSC Adv.* **6**, 5491–5502.
14. T. He, Q. Q. Zeng, D. C. Yang, Y. H. He, and Z. Guan (2015). *RSC Adv.* **5**, 37843–37852.
15. R. Sridhar, B. Srinivas, B. Madhav, V. P. Reddy, Y. V. D. Nageswar, and K. R. Rao (2009). *Can. J. Chem.* **87**, 1704–1707.
16. S. Gao, C. H. Tsai, C. Tseng, and C. F. Yao (2008). *Tetrahedron* **64**, 9143–9149.
17. M. A. Ghasemzadeh, B. Mirhosseini-Eshkevari, and M. H. Abdollahi-Basir (2019). *BMC Chem.* **13**, 119–130.
18. S. E. Sadat-Ebrahimi, S. M. Haghayegh-Zavareh, S. Bahadorikhalili, A. Yahya-Meymandi, M. Mahdavi, and M. Saeedi (2017). *Synth. Commun.* **47**, 2324–2329.
19. M. Taheri, B. Mirza, and M. Zeeb (2018). *J. Nanostruct. Chem.* **8**, 421–429.
20. A. Molla, S. Ranjan, M. S. Rao, A. H. Dar, M. Shyam, V. Jayaprakash, and S. Hussain (2018). *ChemistrySelect* **3**, 8669–8677.
21. A. Ahmadkhani, K. Rad-Moghadam, and S. T. Roudsari (2019). *ChemistrySelect* **4**, 10442–10446.
22. K. Niknam, A. Piran, and Z. Karimi (2016). *J. Iran. Chem. Soc.* **13**, 859–871.
23. M. Baghernejad, S. Khodabakhshi, and S. Tajik (2016). *New J. Chem.* **40**, 2704–2709.
24. S. F. Hojati, A. Amiri, and M. Mahamed (2020). *Res. Chem. Intermed.* **6**, 1091–1107.
25. M. Salavati-Niasari, F. Farzaneh, and M. Ghandi (2016). *J. Mol. Catal. A* **186**, 101–107.
26. D. Ghanbari and M. Salavati-Niasari (2015). *J. Ind. Eng. Chem.* **24**, 284–292.
27. M. Yousefi, F. Gholamian, D. Ghanbari, and M. Salavati-Niasari (2011). *Polyhedron* **30**, 1055–1060.
28. M. Amiri, M. Salavati-Niasari, and A. Akbari (2019). *Adv. Colloid Interface Sci.* **265**, 29–44.
29. A. Abbasi, D. Ghanbari, and M. Salavati-Niasari (2016). *J. Mater. Sci. Mater. Electron.* **27**, 4800–4809.
30. M. Salavati-Niasari, Z. Fereshteh, and F. Davar (2009). *Polyhedron* **28**, 126–130.
31. S. Mortazavi-Derazkola, M. Salavati-Niasari, O. Amiri, and A. Abbasi (2017). *J. Energy Chem.* **26**, 17–23.
32. S. Zinatloo-Ajabshir, M. Salavati-Niasari, and Z. Zinatloo-Ajabshir (2016). *Mater. Lett.* **180**, 27–30.
33. L. Que Jr. (1988). Metal clusters in proteins. *ACS Symp. Ser.* **372**, 152–178.
34. I. C. Gunsalus and S. G. Sligar (1978). *Adv. Enzymol. Relat. Areas Mol. Biol.* **47**, 1.
35. N. Herron (1988). *J. Coord. Chem.* **19**, 25–38.
36. P. P. Knops-Gerrits, D. E. de Vos, and P. A. Jacobs (1997). *J. Mol. Catal. A* **117**, 57–70.
37. M. R. Maurya, C. J. J. Titinchi, and S. Chand (2004). *J. Mol. Catal. A* **214**, 257–264.
38. M. L. Kantam, K. V. S. Ranganath, M. Sateesh, K. B. S. Kumar, and M. B. Choudary (2005). *J. Mol. Catal. A* **225**, 15–20.
39. C. Hardacre, S. P. Katdare, D. Milroy, P. Nancarrow, D. W. Rooney, and J. M. Thompson (2004). *J. Catal.* **227**, 44–52.
40. V. R. Choudhary, S. K. Jana, N. S. Patil, and S. K. Bhargava (2003). *Microporous Mesoporous Mater.* **57**, 21–35.
41. M. Salavati-Niasari (2006). *J. Mol. Catal. A* **245**, 192–199.
42. M. Salavati-Niasari (2005). *Chem. Lett.* **34**, 1444–1445.
43. M. Salavati-Niasari (2008). *J. Mol. Catal. A* **284**, 97–107.
44. M. Moosavifar, A. N. Arbat, Z. Rezvani, and K. Nejati (2015). *Chin. J. Catal.* **36**, 1719–1725.
45. S. F. Hojati, A. Amiri, N. MoeiniEghbali, and S. Mohamadi (2018). *Appl. Organomet. Chem.* **32**, e4235.
46. S. F. Hojati, A. Amiri, S. Mohamadi, and N. MoeiniEghbali (2018). *Res. Chem. Intermed.* **44**, 2275–2287.
47. S. F. Hojati, A. H. Amiri, and H. Raouf (2017). *Appl. Organomet. Chem.* **31**, e3595.
48. S. F. Hojati, N. MoeiniEghbali, S. Mohamadi, and T. Ghorbani (2018). *Org. Prep. Proced. Int.* **50**, 408–415.
49. S. F. Hojati, M. Moosavifar, and T. Ghorbanipoor (2017). *C. R. Chem.* **20**, 520–525.
50. M. Keshavarz, M. Abdoli-Senejani, S. F. Hojati, and Sh. Askari (2018). *React. Kinet. Mech. Cat.* **124**, 757–766.
51. S. F. Hojati and H. Raouf (2016). *Org. Prep. Proced. Int.* **48**, 474–480.
52. S. F. Hojati, A. H. Amiri, and E. Fardi (2020). *Appl. Organomet. Chem.* **34**, e5604.
53. S. F. Hojati, M. Moosavifar, and N. MoeiniEghbali (2020). *J. Chem. Sci.* **132**, 38–46.
54. C. J. Li (2005). *Chem. Rev.* **105**, 3095.
55. F. Bazi, H. El Badaoui, S. Tamani, S. Sokori, A. Solhy, D. J. Macquarrie, et al. (2006). *Appl. Catal. A* **211**, 301–314.
56. B. Sulikowski (1993). *J. Phys. Chem.* **97**, 1420–1425.

57. M. Moosavifar, Sh. Tangestaninejad, M. Moghadam, V. Mirkhani, and I. Mohammadpoor-Baltork (2013). *J. Mol. Catal. A* **377**, 92–101.
58. G. Øye, J. Sjoblom, and M. Stocker (2001). *Adv. Colloid Interface Sci.* **439**, 89–90.
59. M. Moghadam, S. Tangestaninejad, V. Mirkhani, I. Mohammadpoor- Baltork, and M. Moosavifar (2009). *Appl. Catal. A* **358**, 157–163.
60. L.-M. Wang, N. Jiao, J. Qju, J.-J. Yu, F.-L. Guo, and Y. Liu (2010). *Tetrahedron* **66**, 339–343.
61. Md. N. Khan, D. K. Parmar, and H. B. Bhatt (2019). *Asian J. Green Chem.* **3**, 470–482.
62. A. Dandia, A. K. Jain, and D. S. Bhati (2011). *Synth. Commun.* **41**, 2905–2919.
63. C. Wu, R. Shen, J. Chen, and C. Hu (2013). *Bull. Korean Chem. Soc.* **34**, 2431–2435.
64. M. N. Elinson, A. S. Dorofeev, F. M. Miloserdov, and G. I. Nikishi (2009). *Mol. Divers.* **13**, 47–52.